

# Bias in Robust Estimation Caused by Discontinuities and Multiple Structures

Charles V. Stewart, *Member, IEEE*

**Abstract**—When fitting models to data containing multiple structures, such as when fitting surface patches to data taken from a neighborhood that includes a range discontinuity, robust estimators must tolerate both gross outliers and pseudo outliers. Pseudo outliers are outliers to the structure of interest, but inliers to a different structure. They differ from gross outliers because of their coherence. Such data occurs frequently in computer vision problems, including motion estimation, model fitting, and range data analysis. The focus in this paper is the problem of fitting surfaces near discontinuities in range data.

To characterize the performance of least median of the squares, least trimmed squares, M-estimators, Hough transforms, RANSAC, and MINPRAN on this type of data, the “pseudo outlier bias” metric is developed using techniques from the robust statistics literature, and it is used to study the error in robust fits caused by distributions modeling various types of discontinuities. The results show each robust estimator to be biased at small, but substantial, discontinuities. They also show the circumstances under which different estimators are most effective. Most importantly, the results imply present estimators should be used with care, and new estimators should be developed.

**Index Terms**—Robust estimation, outliers, parameter estimation, discontinuities, multiple structures, bias.



## 1 INTRODUCTION

ROBUST estimation techniques have been used with increasing frequency in computer vision applications because they have proven effective in tolerating the gross errors (outliers) characteristic of both sensors and low-level vision algorithms. Most often, robust estimators are used when fitting model parameters—e.g., the coefficients of either a polynomial surface, an affine motion model, a pose estimate, or a fundamental matrix—to a data set. For these applications, robust estimators work reliably when the data contain measurements from a single structure, such as a single surface, plus gross errors.

Sometimes, however, the data are measurements from multiple structures and still corrupted by gross outliers. As two examples, these structures may be different surfaces in depth measurements or multiple moving objects in motion estimation. A difficulty arises because robust estimators are designed to extract a single fit. Thus, to accurately estimate parameters modeling one of the structures—which one is not important—they must treat the points from all other structures as outliers. After successfully estimating the fit parameters of one structure, the robust estimator may be re-applied to estimate subsequent fits after removing the inliers of the first fit from the data.

An example using synthetic range data illustrates the potential problems caused by multiple structures. Fig. 1 shows (nonrobust) linear least-squares fits to data from a single surface and to data from a pair of surfaces forming a

step discontinuity. In the single surface example, the least-squares fit is skewed slightly by the gross outliers, but the fit estimated by a robust version of least-squares will not be significantly corrupted by these outliers. In the multiple surface example, the least-squares fit is skewed so much that it crosses (or “bridges”) the point sets from both surfaces, placing the fit in close proximity to both point sets. Since robust estimators use fit proximity to distinguish inliers and outliers and downgrade the influence of outliers, this raises two concerns about the accuracy of robust fits. First, an estimator that iteratively refines an initial least squares fit will have a local, and potentially global, minimum fit not far from the initial, skewed fit: Points from both surfaces will have both small and large residuals, making it difficult for the estimator to “pull away” from either. Second, and more important, for the robust estimate to be the correct fit, the estimator’s objective function must be lower for the smaller inlier set of the correct fit than the larger inlier set of the bridging fit. By varying both the proximity of the two surfaces and the relative sizes of their point sets, all robust estimators studied here can be made to “fail” on this data, producing fits that are heavily skewed.

Motivated by the foregoing discussion, the goal of this paper is to study how effectively robust estimators can estimate fit parameters given a mixture of data from multiple structures. Stating this “pseudo outliers problem” abstractly, to obtain an accurate fit a robust technique must tolerate two different types of outliers: gross outliers and pseudo outliers. Gross outliers are bad measurements, which may arise from specularities, boundary effects, physical imperfections in sensors, or errors in low-level vision computations such as edge detection or matching algorithms. Pseudo outliers are measurements from one or more additional structures. (Without losing generality,

• The author is with the Department of Computer Science, Rensselaer Polytechnic Institute, Troy, NY 12180-3590.  
E-mail: stewart@cs.rpi.edu.

Manuscript received 11 Mar. 1996. Recommended for acceptance by D.M. Titterton.

For information on obtaining reprints of this article, please send e-mail to: transpami@computer.org, and reference IEEECS Log Number 105206.

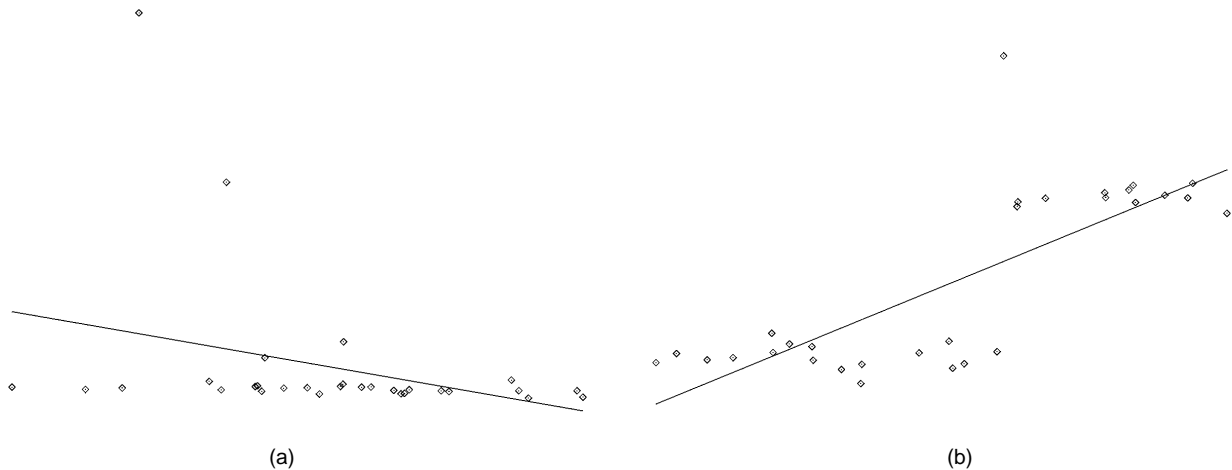


Fig. 1. Examples demonstrating the effects of (a) gross outliers and (b) both gross outliers and data from multiple structures on linear least-squares fits.

inliers and pseudo outliers are distinguished by assuming the inliers are points from the structure contributing the most points, and pseudo outliers are points from the other structures.) The coherence of pseudo outliers distinguishes them from gross outliers. Because data from multiple structures are common in vision applications, the performance of robust estimators on this type of data must be understood to use them effectively.

To study the pseudo outliers problem, this paper develops a measure of “pseudo outlier bias” using tools from the robust statistics literature [10, pp. 81-95] [12, p. 11]. Pseudo outlier bias will measure the distance between a robust estimator’s fit to a “target” distribution and its fit to an outlier corrupted distribution. The target distribution will model the distribution of points drawn from a single structure without outliers, and the outlier corrupted mixture distribution [28] will combine distributions modeling the different structures and a gross outlier distribution. The optimal fit is found by applying the functional form of an estimator to these distributions rather than by applying the standard form of an estimator to particular sets of points generated from these distributions. This gives a theoretical measure, avoids the need for extensive simulations, and, most importantly, shows the *inherent* limitations of robust estimators by studying their objective functions independent of their search techniques. The bias of a number of estimators—M-estimators [12, Chapter 7], least median of squares (LMS) [16], [21], least trimmed squares (LTS) [21], Hough transforms [13], RANSAC [7], and MINPRAN [26]—will be studied as the target and mixture distributions vary.

The application for studying the pseudo outliers problem is fitting surfaces to range data taken from the neighborhood of a surface discontinuity. Since the pseudo outliers problem arises in other applications as well—essentially, any application where the data could contain multiple structures—the results obtained here should be used as qualitative predictions of potential difficulties in these applications. In the context of the range data application, three idealized discontinuity models are used to develop mixture distributions: step edges, crease edges,

and parallel surfaces. Step edges model depth discontinuities, where points from the upper surface of the step are pseudo outliers to the lower surface. Crease edges model surface orientation discontinuities, where points from one side of the crease are pseudo outliers to the other. Finally, parallel surfaces model transparent or semitransparent surfaces, where a background surface appears through breaks in the foreground surface, and data from the background are pseudo outliers to the foreground.

A final introductory comment is important to assist in reading this paper. The paper defines the notion of “pseudo outlier bias” using techniques common in mathematical statistics but not in computer vision, most importantly, the “functional form” of a robust estimator. The intuitive meaning of functional forms and their use in pseudo outlier bias are discussed at the start of Section 4, which then proceeds with the main derivations. Readers uninterested in the mathematical details should be able to skip Sections 4.2 through 4.6 and still follow the analysis results.

## 2 Robust Estimators

This section defines the robust estimators studied. These definitions are converted to functional forms suitable for analysis in Section 4. Because the goal of the paper is to expose inherent limitations of robust estimators, the focus in defining the estimators is their objective functions, rather than their optimization techniques. Special cases of iterative optimization techniques where local minima are potentially problematic will be discussed where appropriate.

The data are  $(\bar{x}_i, z_i)$ , where  $\bar{x}_i$  is an image coordinate vector—the independent variable(s)—and  $z_i$  is a range value—the dependent variable. Each fit is a function  $z = \theta(\bar{x})$ , often restricted to the class of linear or quadratic polynomials. The notation  $\hat{\theta}(\bar{x})$  indicates the fit that minimizes an estimator’s objective function, with  $\hat{\theta}$  called the “estimate.” Each estimator’s objective function evaluates hypothesized fits,  $\theta(\bar{x})$ , via the residuals,  $r_{i,\theta} = z_i - \theta(\bar{x}_i)$ .

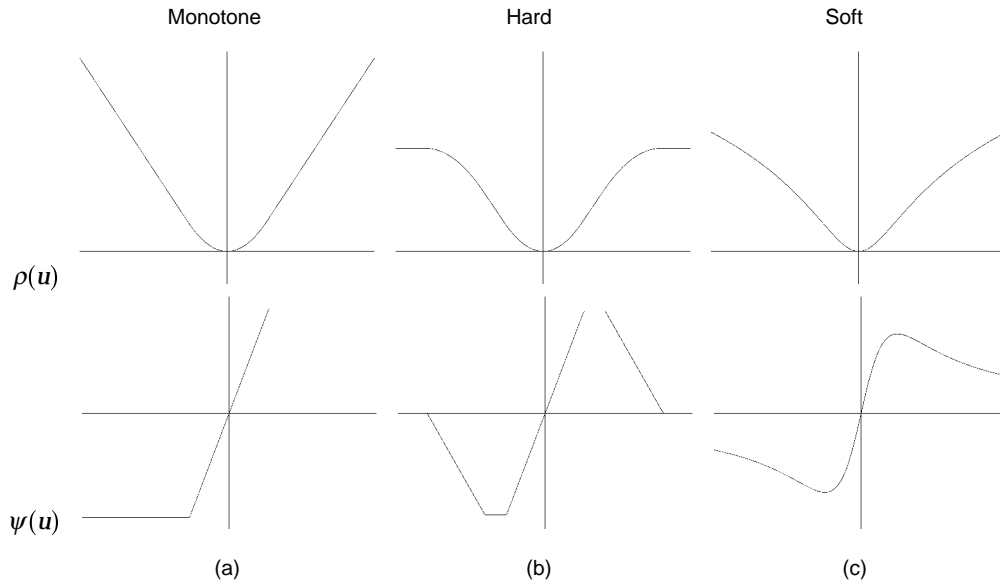


Fig. 2.  $\rho(u)$  and  $\psi(u)$  functions for three M-estimators.

## 2.1 M-Estimators

A regression M-estimate [12, Chapter 7] is

$$\hat{\theta} = \arg \min_{\theta} \sum_i \rho(r_{i,\theta}/\hat{\sigma}), \quad (1)$$

where  $\hat{\sigma}$  is an estimate of the true scale (noise) term,  $\sigma$ , and  $\rho(u)$  is a robust “loss” function which grows subquadratically for large  $|u|$  to reduce the effect of outliers. (Often, as discussed below,  $\hat{\theta}$  and  $\hat{\sigma}$  are estimated jointly.) M-estimators are categorized into three types [11] by the behavior of  $\psi(u) = \rho'(u)$  (the “influence function”); one estimator of each type is studied. *Monotone* M-estimators (Fig. 2a), such as Huber’s [12, Chapter 7], have nondecreasing, bounded  $\psi(u)$  functions. *Hard redescenders* (Fig. 2b), such as Hampel et al.’s [9], [10, p. 150], force  $\psi(u) = 0$  for  $|u| > c$ ; hence,  $c$  is a rejection point, beyond which a residual has no influence. *Soft redescenders* (Fig. 2c), such as the maximum likelihood estimator of Student’s t-distribution [5], do not have a finite rejection point, but force  $\psi(u) \rightarrow 0$  as  $|u| \rightarrow \infty$ . The three robust loss functions are shown in Fig. 2, and, in order, they are

$$\rho_m(u) = \begin{cases} \frac{1}{2} u^2, & |u| \leq c \\ \frac{1}{2} c(2|u| - c), & c < |u| \end{cases} \quad (2)$$

$$\rho_h(u) = \begin{cases} \frac{1}{2} u^2, & |u| \leq a \\ \frac{1}{2} a(2|u| - a), & a < |u| \leq b \\ \frac{1}{2} a \left[ \frac{(|u| - c)^2}{(b - c)} + (b + c - a) \right], & b < |u| \leq c \\ \frac{1}{2} a(b + c - a), & c < |u| \end{cases} \quad (3)$$

and

$$\rho_s(u) = \frac{1}{2} (1 + f) \log(1 + u^2/f) \quad (4)$$

The  $\rho$  function constants are usually set to optimize asymptotic efficiency relative to a given target distribution [11] (e.g., Gaussian residuals).

M-estimators typically minimize  $\sum \rho(r_{i,\theta}/\hat{\sigma})$  using iterative techniques [11] [12, Chapter 7]. The objective functions of hard and soft redescending M-estimators are nonconvex and may have multiple local minima.

In general,  $\hat{\sigma}$  must be estimated from the data. Hard-redescending M-estimators often use the median absolute deviation (MAD) [11] computed from the residuals to an initial fit,  $\hat{\theta}_0$ :

$$\hat{\sigma} = k \operatorname{median}_i \left\{ \left| r_{i,\hat{\theta}_0} - \operatorname{median}_j \{ r_{j,\hat{\theta}_0} \} \right| \right\}, \quad (5)$$

where  $k = 1.4826$  for consistency at the normal distribution and  $k = 1.14601$  for consistency at Student’s t-distribution (when  $f = 1.5$ ). Other M-estimators jointly estimate  $\hat{\sigma}$  and  $\hat{\theta}$  as

$$(\hat{\theta}, \hat{\sigma}) = \arg \min_{\theta, \sigma} \sum_i \rho(r_{i,\theta}, \sigma). \quad (6)$$

In particular, Huber [12, Chapter 7] uses

$$\rho_m(r_{i,\theta}, \sigma) = \left[ \rho_m(r_{i,\theta}/\sigma) + a \right] \sigma, \quad (7)$$

where  $\rho_m(r_{i,\theta}, \sigma)$  is from (2) and  $a$  is a tuning parameter; Mirza et al. [5] use

$$\rho_s(r_{i,\theta}, \sigma) = \ln \sigma + \rho_s(r_{i,\theta}/\sigma), \quad (8)$$

where  $\rho_s(r_{i,\theta}, \sigma)$  is from (4).

When fitting surfaces to range data, a different option for obtaining  $\hat{\sigma}$  is often used [3]. If  $\sigma$  depends only on the properties of the sensor, then  $\hat{\sigma}$  may be estimated once and fixed for all data sets. Theoretically, when  $\hat{\sigma}$  is fixed, the M-estimators described by (1) are no longer true M-estimators since they are not *scale equivariant* [10, p. 259]. To reflect this, when  $\hat{\sigma}$  is fixed a priori, they are called “fixed-scale M-estimators.” Both standard M-estimators and fixed-scale M-estimators are studied here.

## 2.2 Fixed-Band Techniques: Hough Transforms and RANSAC

Hough transforms [13], RANSAC [4], [7], and Roth's primitive extractor [20] are examples of "fixed-band" techniques [20]. For these techniques,  $\hat{\theta}$  is the fit maximizing the number of points within  $\theta \pm r_b$ , where  $r_b$  is an inlier bound which generally depends on  $\hat{\theta}$  (i.e.  $r_b = c\hat{\theta}$  for some constant  $c$ ). Equivalently, viewing fixed-band techniques as minimizing the number of outliers, they become a special case of fixed-scale M-estimators with a simple, discontinuous loss function

$$\rho_f(u) = \begin{cases} 0, & |u| \leq c \\ 1, & |u| > c \end{cases} \quad (9)$$

Fixed-band techniques search for  $\hat{\theta}$  using either random sampling or voting techniques.

## 2.3 LMS and LTS

Least median of squares (LMS), introduced by Rousseeuw [21], finds the fit minimizing the median of squared residuals. (See [16] for a review.) Specifically, the LMS estimate is

$$\hat{\theta} = \arg \min_{\theta} \left\{ \text{median}_i \left\{ \left( r_{i,\theta} \right)^2 \right\} \right\}. \quad (10)$$

Most implementations of LMS use random sampling techniques to find an approximate minimum.

Related to LMS and also introduced by Rousseeuw [21] is the least trimmed squares estimator (LTS). The LTS estimate is

$$\hat{\theta} = \arg \min_{\theta} \sum_{j=1}^h \left( r_{\theta}^2 \right)_{j:N}. \quad (11)$$

where the  $(r_{\theta}^2)_{j:N}$  are the (nondecreasing) ordered squared residuals of fit  $\theta$ . Usually  $h = \lfloor (N+1)/2 \rfloor$ . LTS implementations also use random sampling.

## 2.4 MINPRAN

MINPRAN searches for the fit minimizing the probability that a fit and a collection of inliers to the fit could be due to gross outliers [24], [26]. It is derived by assuming that relative to any hypothesized fit  $\theta(x)$  the residuals of gross outliers are uniformly distributed<sup>1</sup> in the range  $\pm Z_0$ . Based on this assumption, the probability that a particular gross outlier could be within  $\theta(\bar{x}_i) \pm r$  for  $0 \leq r \leq Z_0$  is  $r/Z_0$ . Furthermore, if all  $n$  points are gross outliers, the probability  $k$  or more of them could be within  $\theta(\bar{x}) \pm r$  is

$$\mathcal{F}(r, k, n) = \sum_{j=k}^n \binom{n}{j} \left( r/Z_0 \right)^j \left( 1 - r/Z_0 \right)^{n-j}. \quad (12)$$

Given  $n$  data points containing an unknown number of gross outliers, MINPRAN evaluates hypothesized fits  $\theta(\bar{x})$  by finding the inlier bound,  $r$ , and the associated number of points (inliers),  $k_{r,\theta}$ , within  $\pm r$  of  $\theta(\bar{x})$ , minimizing the probability that the inliers could actually be gross outliers. Thus MINPRAN's objective function in evaluating a particular fit is

$$\min_r \mathcal{F}(r, k_{r,\theta}, n)$$

and MINPRAN's estimate is

$$\hat{\theta} = \arg \min_{\theta} \left[ \min_r \mathcal{F}(r, k_{r,\theta}, n) \right]. \quad (13)$$

MINPRAN is implemented using random sampling techniques (see [26]).

## 3 MODELING DISCONTINUITIES

The important first step in developing the pseudo outlier bias analysis technique is to model the data taken from near a discontinuity as a probability distribution. Attention here is restricted to discontinuities in one-dimensional structures, since this will be sufficient to demonstrate the limitations of robust estimators.

### 3.1 Outlier Distributions

To set the context, consider the one-dimensional, outlier corrupted distributions used to study robust location estimators [10, p. 97] [12, p. 11]:

$$F = (1 - \varepsilon) F_1 + \varepsilon G$$

Here,  $F_1$  is an inlier distribution (a "target distribution"), such as a unit variance Gaussian, and  $G$  is an outlier distribution, such as a large variance Gaussian or a uniform distribution over a large interval. The parameter  $\varepsilon$  is the outlier proportion. A set  $A$  of  $N$  points sampled from this distribution will contain, on average,  $\varepsilon N$  outliers. Robust location estimators may be analyzed using distribution  $F$ , rather than using a series of point sets sampled from  $F$ .

### 3.2 Mixture Distributions Modeling Discontinuities

The present paper analyzes robust regression estimators by examining their behavior on distributions modeling discontinuities. These mixture distributions [28] will be of the form

$$H = (1 - \varepsilon_o) [\varepsilon_s H_1 + (1 - \varepsilon_s) H_2] + \varepsilon_o H_o \quad (14)$$

$H_1$ ,  $H_2$ , and  $H_o$  will be inlier, pseudo outlier, and gross outlier distributions, respectively, and  $\varepsilon_s$  and  $\varepsilon_o$  will control the proportion of points drawn from the three distributions.

To formulate  $H_1$ ,  $H_2$ , and  $H_o$  and to set  $\varepsilon_s$  and  $\varepsilon_o$ , consider a set,  $S$ , of data points taken from the vicinity of a discontinuity. For example,  $S$  might contain the points in Fig. 3 whose  $x$  coordinates fall in the interval  $[x_0, x_1]$ .  $H_1$  is modeled as a two-dimensional distribution of points  $(x, z)$  with  $x$  values in an interval  $[x_0, x_d]$ —assuming, without losing generality, more points are from the left side of the discontinuity location than the right. (Using a two-dimensional distribution might be counterintuitive since the  $x$  values, which may be thought of as image positions at which measurements are recorded, are usually fixed.) Here,  $x$  is treated as uniform in the interval  $[x_0, x_d]$ , modeling the uniform spacing of image positions.<sup>2</sup> The measurement for an

2. For any point set sampled from this distribution, the  $x$  values will not be uniformly spaced, in general, but the expected values of their order statistics are. This expected behavior is captured when using the distribution itself in the analysis rather than points sets sampled from the distribution.

1. MINPRAN has been generalized to any known outlier distribution [26].

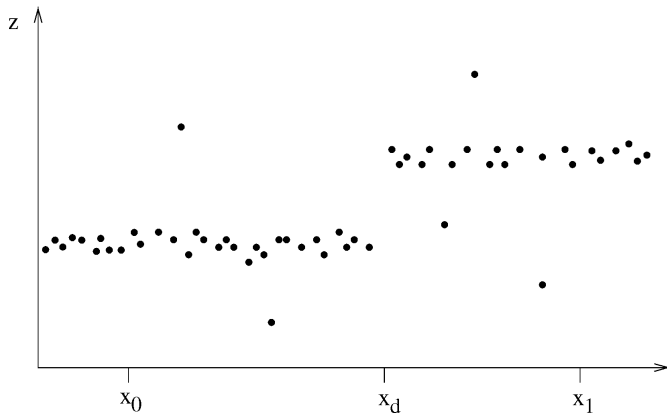


Fig. 3. Example data set for points near a step discontinuity.

inlier is  $z = \beta_1(x) + e$ , where  $e$  is independent noise controlled by the Gaussian density  $g(0; \sigma^2)$ . The pseudo outlier distribution,  $H_2$ , may be defined similarly, with  $x$  values uniform in  $[x_d, x_1]$  and measurements  $z = \beta_2(x) + e$ . Thus, for both distributions  $H_1$  and  $H_2$ , the densities of  $x$  and  $z$  can be combined to give the joint density

$$h_i(x, z) = \begin{cases} \frac{g(z - \beta_i(x); \sigma^2)}{x_{i,1} - x_{i,0}}, & x_{i,0} \leq x \leq x_{i,1} \\ 0, & \text{otherwise.} \end{cases} \quad (15)$$

where  $i \in \{1, 2\}$  and  $x_{i,0}$  and  $x_{i,1}$  bound the uniform distribution on the  $x$  interval.

For  $H_o$ , the distribution of gross outliers in  $S$ , again  $x$  values are uniformly distributed, but this time over the entire interval  $[x_0, x_1]$ , and  $z$  values are governed by density  $g_o(z)$ , which will be uniform over a large range. This gives the joint density for a gross outlier:

$$h_o(x, z) = \begin{cases} \frac{g_o(z)}{x_1 - x_0}, & x_0 \leq x \leq x_1 \\ 0, & \text{otherwise.} \end{cases} \quad (16)$$

The mixture proportions  $\varepsilon_s$  and  $\varepsilon_o$  in (14) are easily specified.  $\varepsilon_o$  is just the fraction of gross outliers.  $\varepsilon_s$  is the “relative fraction” of inliers, i.e., the fraction points that are not gross outliers and that are from the inlier side of the discontinuity. Assuming the density of  $x$  values does not change across the discontinuity,  $\varepsilon_s$  is determined by  $x_d$ :

$$\varepsilon_s = \frac{x_d - x_0}{x_1 - x_0}. \quad (17)$$

Equivalently, given  $\varepsilon_s$ ,  $x_d = x_0 + \varepsilon_s(x_1 - x_0)$ . (To distinguish inliers and pseudo outliers, assume  $\varepsilon_s > 0.5$ .) Notice that the “actual fraction” of inliers is  $\varepsilon_1 = (1 - \varepsilon_o)\varepsilon_s$ . Depending on which estimator is being analyzed, either the relative or the actual fraction or both will be important.

Using these mixture proportions, the above densities can be combined into a single, mixed, two-dimensional density:

$$h(x, z) = (1 - \varepsilon_o)[\varepsilon_s h_1(x, z) + (1 - \varepsilon_s) h_2(x, z)] + \varepsilon_o h_o(x, z). \quad (18)$$

Observe that the “target density” is just  $h_1(x, z)$  and the “target distribution” is  $H_1(x, z)$ . The mixture distribution  $H(x, z)$  and the target distribution  $H_1(x, z)$  can be calculated from  $h(x, z)$  and  $h_1(x, z)$ , respectively.

Using mixture density  $h(x, z)$ , data can be generated to form step edges and crease edges. The appropriate model is determined by the two curve functions  $\beta_1$  and  $\beta_2$ . For example, a step edge of height  $\Delta z$  is modeled by setting  $\beta_1(x) = c$  and  $\beta_2(x) = c + \Delta z$ , for some constant  $c$ . A crease edge is modeled when  $\beta_1$  and  $\beta_2$  are linear functions and  $\beta_1(x_d) = \beta_2(x_d)$ . Parallel lines with overlapping  $x$  domains can be created by using  $\beta_1$  and  $\beta_2$  from step edges, but setting  $x_{1,0} = x_{2,0} = x_0$  and  $x_{1,1} = x_{2,1} = x_1$ , and letting  $\varepsilon_s$  represent the proportion of points from the lower line. In this case, the mixture proportions are divorced from the location of the discontinuity, which has no meaning. Thus, all three desired discontinuities can be modeled.

## 4 FUNCTIONAL FORMS AND MIXTURE MODELS

To analyze estimators on distributions  $H$ , each estimator must be rewritten as a functional,  $T$ —a mapping from the space of probability distributions to the space of possible estimates.

This section derives functional forms of the robust estimators defined in Section 2. It starts, in Section 4.1, by giving intuitive insight. Then, Section 4.2 introduces functional forms and empirical distributions on a technical level, using univariate least-squares location estimates as an example. Next, Section 4.3 derives several important distributions needed in the functionals. The remaining sections derive the required functionals. Readers uninterested in the technical details should read only Section 4.1 and then skip ahead to Section 5.

### 4.1 Intuition

To illustrate what it means for a functional  $T$  to be applied to a distribution  $H$ , consider least-squares regression. When applied to a set containing points  $(x_i, z_i)$ , the least-squares objective function is

$$\sum_i [z_i - \theta(x_i)]^2 = \sum_i r_{i,\theta}^2,$$

which is proportional to the second moment of the residuals conditioned on  $\theta$ . The least squares estimate is the fit  $\hat{\theta}$  minimizing this conditional second moment. A similar second moment, conditioned on  $\theta$ , can be calculated for distribution  $H(x, z)$ , and the fit  $\hat{\theta}$  minimizing this conditional second moment can be found. This is the least-squares regression functional. The functional form of an M-estimator, by analogy, returns the fit minimizing a robust version of the second moment of the conditional residual distribution calculated from  $H$ . Intuitions about the functional forms of other estimators are similar.

The estimate  $T(H)$  can be used to represent or characterize the estimator’s performance on point sets sampled from  $H$ . Although the robust fit to any particular point set may differ from  $T(H)$ , if  $T(H)$  is skewed by the pseudo and gross outliers, then the fit to the point set will likely be skewed as

well. Indeed, when an estimator’s minimization technique is an iterative search, the skew may be worse than that of  $T(H)$  because of local minima.

**4.2 One-Dimensional Location Estimators**

To introduce functional forms on a more technical level, this section examines the least-squares location estimate for univariate data. For a finite sample  $\{x_1, \dots, x_n\}$ , the location estimate is

$$\hat{\theta} = \arg \min_{\theta} \frac{1}{n} \sum_i (x_i - \theta)^2 = \frac{1}{n} \sum_i x_i, \tag{19}$$

which is the sample mean or expected value. The functional form of this is the location estimate of the distribution  $F$ , from which the  $x_i$ s are drawn:

$$\begin{aligned} T_{loc}(F) &= \hat{\theta} \\ &= \arg \min_{\theta} \int (x - \theta)^2 dF \\ &= \arg \min_{\theta} \int (x - \theta)^2 f(x) dx \\ &= \int x f(x) dx, \end{aligned} \tag{20}$$

the population mean or expected value.

The functional form of the location estimate is derived from the sample location estimate by writing the latter in terms of the “empirical distribution” of the data, denoted by  $F_n$ , and then replacing  $F_n$  with  $F$ , the actual distribution. The *empirical density* of  $\{x_1, \dots, x_n\}$  is

$$f_n(x) = \frac{1}{n} \sum_i \delta(x - x_i).$$

where  $\delta(\cdot)$  is the Dirac delta function, and the *empirical distribution* is

$$F_n(x) = \frac{1}{n} \sum_i u(x - x_i),$$

where  $u(\cdot)$  is the unit step function. When the  $x_i$ s are independent and identically distributed,  $F_n$  converges to  $F$  as  $n \rightarrow \infty$ . The least squares location estimate is written in terms of the empirical density by using the sifting property of the delta function [8, p. 56]:

$$\begin{aligned} \arg \min_{\theta} \frac{1}{n} \sum_i (x_i - \theta)^2 &= \arg \min_{\theta} \frac{1}{n} \sum_i \int (x - \theta)^2 \delta(x - x_i) dx \\ &= \arg \min_{\theta} \int (x - \theta)^2 \frac{1}{n} \sum_i \delta(x - x_i) dx \\ &= \arg \min_{\theta} \int (x - \theta)^2 f_n(x) dx \end{aligned}$$

Replacing  $f_n$  with the population density  $f(x) = dF/dx$  yields the functional form of the location estimate as desired (20).

**4.3 Residual Distributions and Empirical Distributions**

Before deriving functional forms for the robust regression estimators, the mixture distribution  $H(x, z)$  must be rewritten in terms of the distribution of residuals relative to a hypothesized fit,  $\theta$ . This is because the objective functions of

the estimators depend directly on residuals  $r$ , and only indirectly on points  $(x, z)$ . In addition, several empirical versions of this “residual distribution” are needed.

Two different residual distributions are required: one for signed residuals and one for their absolute values. Let the distribution and density of signed residuals be  $F^s(r|\theta, H)$  and  $f^s(r|\theta, H)$  (including  $H$  in the notation to make explicit the dependence on the mixture distribution). These are found by integrating the mixture density over the region enclosed by the dashed lines in Fig. 4a:

$$F^s(r|\theta, H) = \int_{x_0}^{x_1} \int_{-\infty}^{\theta(x)+r} h(x, z) dz dx, \tag{21}$$

and

$$f^s(r|\theta, H) = dF^s(r|\theta, H)/dr = \int_{x_0}^{x_1} h(x, \theta(x) + r) dx. \tag{22}$$

Let the distribution and density of absolute residuals be  $F^a(r|\theta, H)$  and  $f^a(r|\theta, H)$ , where  $r \geq 0$ . These are found by integrating the mixture density over the region enclosed by the dashed lines in Fig. 4b:

$$F^a(r|\theta, H) = \int_{x_0}^{x_1} \int_{\theta(x)-r}^{\theta(x)+r} h(x, z) dz dx, \tag{23}$$

and

$$\begin{aligned} f^a(r|\theta, H) &= dF^a(r|\theta, H)/dr \\ &= \int_{x_0}^{x_1} [h(x, \theta(x) + r) + h(x, \theta(x) - r)] dx. \end{aligned} \tag{24}$$

Details of evaluating these integrals may be found in the appendix of [27], which is available on the world-wide web.

Replacing  $h$  with  $h_i$  in the above equations yields the residual distributions and densities for the target (inlier) distribution.

Now, several empirical distributions are needed below. First, given  $n$  points  $(x_i, z_i)$  sampled from  $h(x, z)$ , the empirical density of the data is simply

$$h_n(x, z) = \frac{1}{n} \sum_i \delta(x - x_i, z - z_i).$$

( $h_n$  should not be confused with  $h_i$  from (15).) Next, the empirical density of the signed residuals follows from  $h_n(x, z)$  using the sifting property of the  $\delta$  function [8, p. 56]:

$$\begin{aligned} f_n^s(r|\theta, H_n) &= \int_{-\infty}^{\infty} h_n(x, \theta(x) + r) dx \\ &= \frac{1}{n} \sum_i \delta(\theta(x_i) + r - z_i) \end{aligned} \tag{25}$$

Finally, the empirical distribution of the absolute residuals is

$$F_n^a(r|\theta, H_n) = \int_{-r}^r f_n^s(y|\theta) dy. \tag{26}$$

**4.4 M-Estimators and Fixed-Band Techniques**

The functionals for the robust regression estimators can now be derived, starting with that of fixed-scale M-estimators. The first step is to write (1) in a slightly modified form, which does not change the estimate:

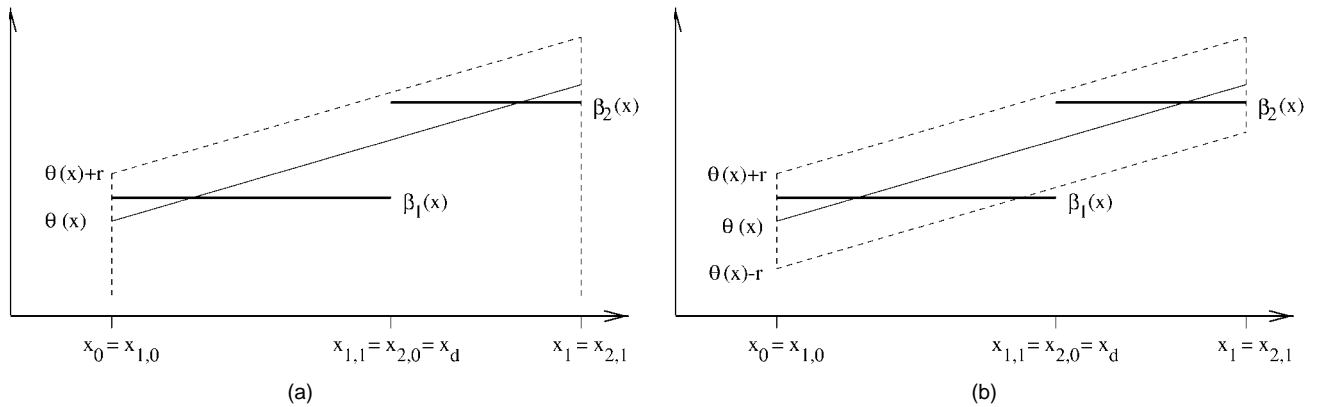


Fig. 4. The dashed lines enclose the regions of integration for calculating the cumulative distribution of signed (a) and absolute (b) residuals  $r$  relative to fit  $\theta(x)$ .

$$\hat{\theta} = \arg \min_{\theta} \frac{1}{n} \sum_i \rho(r_{i,\theta}/\hat{\sigma}).$$

Next, writing this in terms of the empirical distribution produces

$$\begin{aligned} \arg \min_{\theta} \frac{1}{n} \sum_i \rho(r_{i,\theta}/\hat{\sigma}) &= \arg \min_{\theta} \frac{1}{n} \sum_i \rho((z_i - \theta(x_i))/\hat{\sigma}) \\ &= \arg \min_{\theta} \frac{1}{n} \sum_i \iint \rho((z - \theta(x))/\hat{\sigma}) \delta(x - x_i, z - z_i) dx dz \\ &= \arg \min_{\theta} \iint \rho((z - \theta(x))/\hat{\sigma}) h_n(x, z) dx dz. \end{aligned}$$

Replacing the empirical density  $h_n(x, z)$  with the mixture density  $h(x, z)$  yields

$$T_{\rho}(H) = \arg \min_{\theta} \iint \rho((z - \theta(x))/\hat{\sigma}) h(x, z) dx dz.$$

The change of variables  $r = z - \theta(x)$  simplifies things further:

$$T_{\rho}(H) = \arg \min_{\theta} \int \rho(r/\hat{\sigma}) f^s(r|\theta, H) dr. \quad (27)$$

This is the fixed-scale M-estimator functional. Substituting (2), (3), and (4) gives functionals  $T_{\rho_m}$ ,  $T_{\rho_h}$ , and  $T_{\rho_s}$ , respectively, for the M-estimators studied here.

For the M-estimators that jointly estimate  $\hat{\theta}$  and  $\hat{\sigma}$  (see (7) and (8)), the functional is obtained by replacing  $\rho(r/\hat{\sigma})$  with  $\rho(r, \sigma)$  in (27), producing

$$T_{\rho,s}(H) = \arg \min_{\theta} \min_{\sigma} \int \rho(r/\sigma) f^s(r|\theta, H) dr. \quad (28)$$

Finally, recalling that fixed-band techniques (see Section 2.2) are special cases of fixed-scale M-estimators, their functional is obtained by substituting (9) into (27), yielding

$$\begin{aligned} T_b(H) &= \arg \min_{\theta} \left[ \int_{-\infty}^{-r_b} f^s(r|\theta, H) dr + \int_{r_b}^{\infty} f^s(r|\theta, H) dr \right] \\ &= \arg \min_{\theta} [1 - F^a(r_b|\theta, H)]. \end{aligned} \quad (29)$$

Observe that  $[1 - F^a(r_b|\theta, H)]$  is the expected fraction of outliers.

#### 4.5 LMS and LTS

Deriving the functional equivalent to LMS requires first deriving the cumulative distribution of the squared residuals and then writing the median in terms of the inverse of this distribution. Defining  $y = r^2$ , the empirical distribution of squared residuals is

$$F_{n,y}(y|\theta, H) = F_n^a(\sqrt{y}|\theta, H),$$

since it is simply the percentage of points whose absolute residuals relative to fit  $\theta$  are less than  $\sqrt{y}$ . Now,

$$\text{median}\{r_{i,\theta}^2\} = F_{n,y}^{-1}(1/2|\theta, h). \quad (30)$$

In other words, the median is the inverse of the cumulative, evaluated at 1/2. Substituting (30) in (10) and replacing the empirical distribution  $F_{n,y}$  with  $F_y(y|\theta, H) = F^a(\sqrt{y}|\theta, H)$  produces the LMS functional:

$$T_L(H) = \arg \min_{\theta} F_y^{-1}(1/2|\theta, H). \quad (31)$$

Turning now to LTS, normalizing its objective function and writing it in terms of the empirical density of residuals yields

$$\frac{1}{n} \sum_{j=1}^{\lfloor (N+1)/2 \rfloor} (r_{\theta}^2)_{j,N} = \int_{-r_m}^{r_m} r^2 f_n^s(r|\theta, H_n) dr$$

where  $r_m^2 = F_{n,y}^{-1}(1/2|\theta, H_n)$  is the empirical median square residual. The functional form of LTS then is easily written as

$$T_T(H) = \arg \min_{\theta} \int_{-F_y^{-1}(1/2|\theta, H)}^{F_y^{-1}(1/2|\theta, H)} r^2 f^s(r|\theta, H) dr. \quad (32)$$

#### 4.6 MINPRAN

MINPRAN's functional is derived by first rewriting MINPRAN's objective function, replacing the binomial distribution with the incomplete beta function [19, p. 229]:

$$\min_r \mathcal{F}(r, k_{r,\theta}, n) = \min_r I(k_{r,\theta}, n - k_{r,\theta} + 1, r/Z_0)$$

where

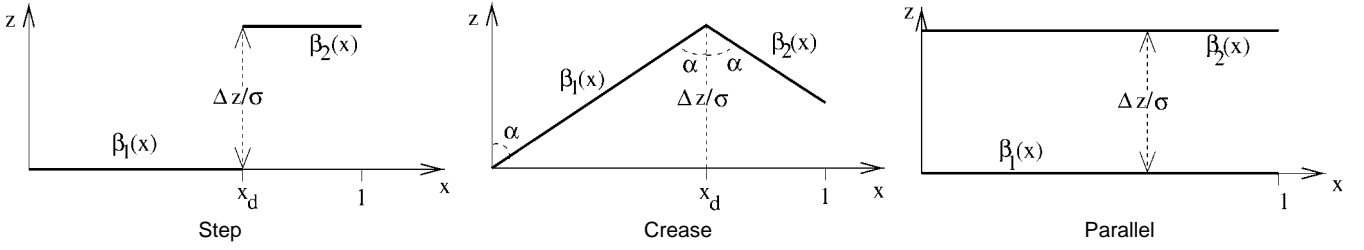


Fig. 5. Parameters controlling the curve models for step edges, crease edges, and parallel lines. In each case,  $\beta_1(x)$  is the desired correct fit and points from  $\beta_2(x)$  are pseudo outliers.  $\Delta z/\sigma$  is the scaled discontinuity magnitude, and  $\varepsilon_s$  controls the percentage of points from  $\beta_1(x)$ .

$$I(v, w, p) = \frac{\Gamma(v+w)}{\Gamma(v)\Gamma(w)} \int_0^p t^{v-1}(1-t)^{w-1} dt.$$

and  $\Gamma(\cdot)$  is the gamma function. This is done because  $I(v, w, p)$  only requires  $v, w \in \mathfrak{R}^+$ , whereas the binomial distribution requires integer values for  $k_{r,\theta}$  and  $n$ . Now, since  $F_n^a(r|\theta, H_n)$  is the empirical distribution of the absolute residuals (see (26)),  $k_{r,\theta} = n \cdot F_n^a(r|\theta, H_n)$  for all  $r > 0$ . Thus, MINPRAN's objective function can be rewritten equivalently as

$$\min_r I(n \cdot F_n^a(r|\theta, H_n), n(1 - F_n^a(r|\theta, H_n)) + 1, r/Z_0),$$

Replacing  $F_n^a$  by  $F^a$ , and substituting (13), gives the functional

$$T_M(H) = \arg \min_{\theta} \left\{ \min_r I(n \cdot F^a(r|\theta, H), n(1 - F^a(r|\theta, H)) + 1, r/Z_0) \right\}. \quad (33)$$

Observe that  $n$ , the number of points, is still required here, but  $T_M(H)$  is considered a functional [10, p. 40].

## 5 PSEUDO OUTLIER BIAS

Now that the functional forms of the robust estimators have been derived, the pseudo outlier bias metric can be defined. Given a particular mixture distribution  $H(x, z)$ , target distribution  $H_1(x, z)$ , and a functional  $T$ , let

$$\hat{\theta} = T(H) \text{ and } \hat{\theta}_1 = T(H_1).$$

These fits are assumed to minimize the estimator's objective functional globally. Then, pseudo outlier bias is defined as the normalized  $L^2$  distance between the fits:

$$\|\hat{\theta} - \hat{\theta}_1\|_2 = \frac{1}{(x_1 - x_0)} \left\{ \int_{x_0}^{x_1} \left[ \frac{\hat{\theta}(x) - \hat{\theta}_1(x)}{\sigma} \right]^2 dx \right\}^{1/2}. \quad (34)$$

As is easily shown, this metric on the estimates is invariant to translation and independent scaling of both  $x$  and  $z$ . (For fixed-scale M-estimators,  $\hat{\sigma}$ , which is provided a priori, must be scaled as well. For MINPRAN, the outlier distribution must be scaled appropriately.)

When the set of the possible curves  $\theta(x)$  includes  $\beta_1(x)$ , it can be shown that, for each of the functionals derived in Section 4,  $T(H_1) = \hat{\theta}_1 = \beta_1$ . In other words, the objective function of the estimator is minimized by  $\beta_1$ . When  $T(H) = \beta_1$ , the pseudo outlier bias metric becomes

$$\|\hat{\theta} - \beta_1\|_2 = \frac{1}{(x_1 - x_0)} \left\{ \int_{x_0}^{x_1} \left[ \frac{\hat{\theta}(x) - \beta_1(x)}{\sigma} \right]^2 dx \right\}^{1/2}. \quad (35)$$

Intuitively, pseudo outlier bias measures the  $L^2$  norm distance between the two estimates,  $T(H)$  and  $T(H_1)$ , normalized by the length of the  $x$  interval  $[x_0, x_1]$  and by the standard deviation,  $\sigma$ , of the noise in the  $z$  values. Since  $T(H_1) = \beta_1$  for the cases studied here, a metric value of 0 implies that  $T$  is not at all corrupted by the presence of either gross or pseudo outliers, and a metric value of 1 implies that on average over the  $x$  domain  $T(H)$  is one standard deviation away from  $\beta_1$ .

## 6 BIAS CAUSED BY SURFACE DISCONTINUITIES

Pseudo outlier bias (or "bias" for short) can now be used to analyze the accuracy of robust estimators in fitting surfaces to data from three different types of discontinuities: step edges, crease edges, and parallel lines with overlapping  $x$  domains. To do this, Section 6.1 parameterizes the mixture density, outlines the technique to find  $T(H)$ , and discusses the relationship between results presented here and results for higher dimensions. Then, numerical results for specific estimators are presented: fixed-scale M-estimators and fixed-band techniques (Section 6.2) which require a prior estimate of  $\hat{\sigma}$ , standard M-estimators (Section 6.3) which estimate  $\hat{\sigma}$ , and LMS, LTS, and MINPRAN (Section 6.4) whose objective functions are independent of  $\hat{\sigma}$ . In each case, the bias is examined as both the discontinuity magnitude and mixture of inliers, pseudo outliers and gross outliers vary.

### 6.1 Discontinuity Models and Search

Fig. 5 shows the models of step edges, crease edges, and parallel lines. The translation and scale invariance of both the estimators and pseudo outlier bias, along with several realistic assumptions, allow these discontinuities to be described with just a few parameters. (Refer back to Section 3 for the exact parameter definitions.) For all models,  $\sigma = 1.0$  and the  $x$  interval is  $[0, 1]$ . For step edges,  $\beta_1(x) = 0$  and  $\beta_2(x) = \Delta z/\sigma$ —retaining the  $\sigma$  parameter to make clear the scale invariance—and  $x_{1,0} = 0$ ,  $x_{2,1} = 1$ , and  $x_{1,1} = x_{2,0} = x_d$ . With these values,  $\varepsilon_s = x_d$ . To move from step to crease edges, only the curves  $\beta_1(x)$  and  $\beta_2(x)$  must be changed. Referring to Fig. 5b, these functions are  $\beta_1(x) = (\Delta z/\sigma)(x/x_d)$  and  $\beta_2(x) = (\Delta z/\sigma)(-x/x_d + 2)$ . Note  $\alpha$  plays no explicit role because it is not scale invariant. For parallel lines (Fig. 5c),  $\beta_1(x)$  and  $\beta_2(x)$  are the same as for step edges,  $x_{1,0} = x_{2,0} = 0$  and  $x_{1,1} = x_{2,1} = 1$ , and the parameter  $x_d$  plays no role. Finally, the outlier distribution  $g_o(z)$  is defined to be uniform for  $z$  within  $\pm z_0/2$ , of  $\Delta z/2$  and 0, otherwise.

The foregoing shows that the parameters  $\varepsilon_s$ ,  $\varepsilon_o$ ,  $\Delta z/\sigma$ , and  $z_0$  completely specify a two curve discontinuity model,



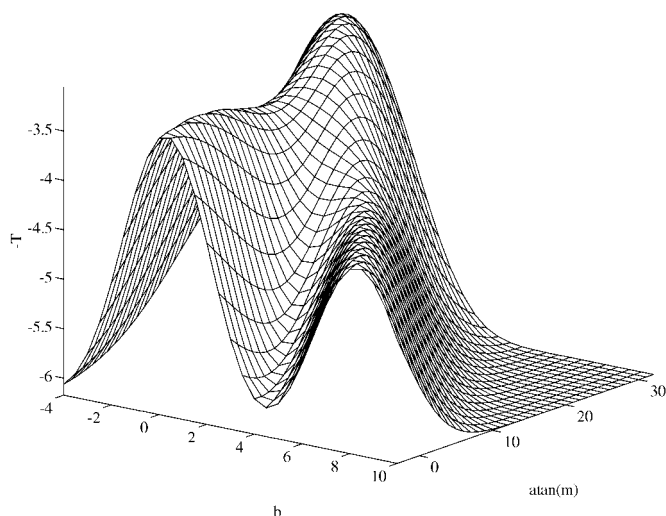


Fig. 6. Surface plot of the objective functional  $T_{\rho_h}(H)$  on a step edge with  $\varepsilon_s = 0.6$  and  $\Delta z/\sigma = 7.5$  when fits have the form  $\theta(x) = mx + b$ . (The plot shows the negation of the objective functional.) There are three local optimal: one at  $\theta(x) = \beta_1(x)$ , the second at  $\theta(x) = \beta_2(x)$ , and the third at a heavily biased fit,  $\theta(x) = \tan(27.92^\circ)x - 1.91$ . The biased fit is the global optimum.

the resulting mixture density,  $h(x, z)$ , and, therefore, the distribution,  $H(x, z)$ . Hence, after specifying the class of functions (linear, here) for hypothesized fits, a given robust estimator's pseudo outlier bias can be calculated as a function of these parameters. This calculation requires an iterative, numerical search to minimize  $T(H)$ , and may require several starting points to avoid local minima. (See Fig. 6 for an example plot of  $T_{\rho_h}$ .) Thus, for a particular type of discontinuity and for a particular robust estimator, the parameters may be varied to study their effect on the estimator's pseudo outlier bias, thereby characterizing how accurately the estimator can fit surfaces near discontinuities.

As a final observation, although the results are presented for one-dimensional image domains, they have immediate extension to two dimensions. For example, a two-dimensional analog of the step edge presented here is  $\beta_1(x, y) = 0$  for  $x \in [0, x_d]$  and  $y \in [0, 1]$  and  $\beta_2(x, y) = \Delta z/\sigma$  for  $x \in [x_d, 1]$  and  $y \in [0, 1]$ . It is straightforward to show that this model results in exactly the same pseudo outlier bias as a one-dimensional step model having the same mixture parameters and gross outlier distribution. Similar results are obtained for natural extensions of the crease edge and parallel lines models. Thus, one-dimensional discontinuities are sufficient to establish limitations in the effectiveness of robust estimators.

## 6.2 Fixed-Scale M-Estimators and Fixed-Band Techniques

The first numerical results are for fixed-band techniques and fixed-scale M-estimators. These techniques represent an ideal case where the noise parameter  $\hat{\sigma} = \sigma$  is known and fixed in advance. Fig. 7 shows the bias of fixed-band techniques ( $T_f$ ) and three fixed-scale M-estimators ( $T_{\rho_m}$ ,  $T_{\rho_s}$ , and  $T_{\rho_h}$ ) as a function  $\Delta z/\sigma$  when  $\varepsilon_s = 0.6$  and when  $\varepsilon_s = 0.8$ . The bias of the least-squares estimator, calculated by substituting  $\rho(u) = u^2$  into (27), is included for comparison. The

$\rho$  function tuning parameters values are directly from the literature ( $c = 1.345$  for  $\rho_m$  [11],  $a = 1.31$ ,  $b = 2.04$ ,  $c = 4.00$  for  $\rho_h$  [10, p. 167],  $f = 1.5$  for  $\rho_s$  [18]), and  $r_b = 2.5\hat{\sigma}$  for  $T_b$ . Interestingly, the proportion of gross outliers,  $\varepsilon_o$ , has no effect on the results. This is because the fraction of the outlier distribution within  $r$  of a fit is the same for all fits  $\theta$  and for all  $r$ , except when  $\theta(x) \pm r$  is extreme enough to cross outside the bounds of the gross outlier distribution.

The sharp drops in bias shown in Figs. 7a and 7b for fixed-band techniques and for the hard redescending M-estimator (and to some extent for the soft redescending M-estimator in (b)) correspond to  $\hat{\theta}(x) = T_\rho(H)$ , shifting from the local minimum associated with a heavily biased fit to the local minimum near  $\beta_1(x)$ , the optimum fit to the target distribution. Plotting the step height at which this drop occurs as a function of  $\varepsilon_s$  gives a good summary of the bias of these estimators on step edges. Fig. 8 does this, referring to this height as the "small bias height" and quantifying it as the step height at which the bias drops below 1.0.

The plots in Figs. 7 and 8a show that fixed-band techniques and fixed-scale M-estimators are biased nearly as much as least-squares for significant step edge and crease edge discontinuity magnitudes. The estimators fare much better on parallel lines (Figs. 7e and 7f); apparently, asymmetric positioning of pseudo outliers causes the most bias. To give an intuitive feel for the significance of the bias, Fig. 9 shows step edge data generated using  $\varepsilon_s = 0.6$  and  $\Delta z/\sigma = 7.5$ , model parameters for which the robust estimators are strongly biased.

Overall, the hard redescending, fixed-scale M-estimator is the least biased of the techniques studied thus far. Compared to other fixed-scale M-estimators, its finite rejection point—the point at which outliers no longer influence the fit—makes it less biased by pseudo outliers than monotone and soft redescending fixed-scale M-estimators. On the other hand, it is less biased than fixed-band techniques<sup>3</sup> because it retains the statistical efficiency of least-squares for small residuals.

The hard redescending, fixed-scale M-estimator can be made less biased by reducing the values of its tuning parameters, as shown in Fig. 8b, effectively narrowing  $\rho_h$  and reducing its finite rejection point. (The parameter set  $a = 1.0$ ,  $b = 1.0$ ,  $c = 2.0$  comes from [2]; the set  $a = 1.0$ ,  $b = 2.0$ ,  $c = 3.0$  was chosen as an intermediate set of values.) Using small parameter values has two disadvantages, however: The optimum statistical efficiency of the standard parameters is lost, giving less accurate fits to the target distribution, and some good data may be rejected as outliers. Despite these disadvantages, lower tuning parameters should be used since avoiding heavily biased fits is the most important objective.

Finally, in practice, the nonconvex objective functions of hard and soft redescending fixed-scale M-estimators can lead to more biased results than indicated here. Iterative search techniques, especially when started from a nonrobust fit, may stop at a local minimum corresponding to a biased fit when the fit to the target distribution is the global

3. When interpreting the results for Hough transforms, a type of fixed-band technique, be aware that  $T_b(H) = \hat{\theta}$  corresponds to the peak position in transform space.

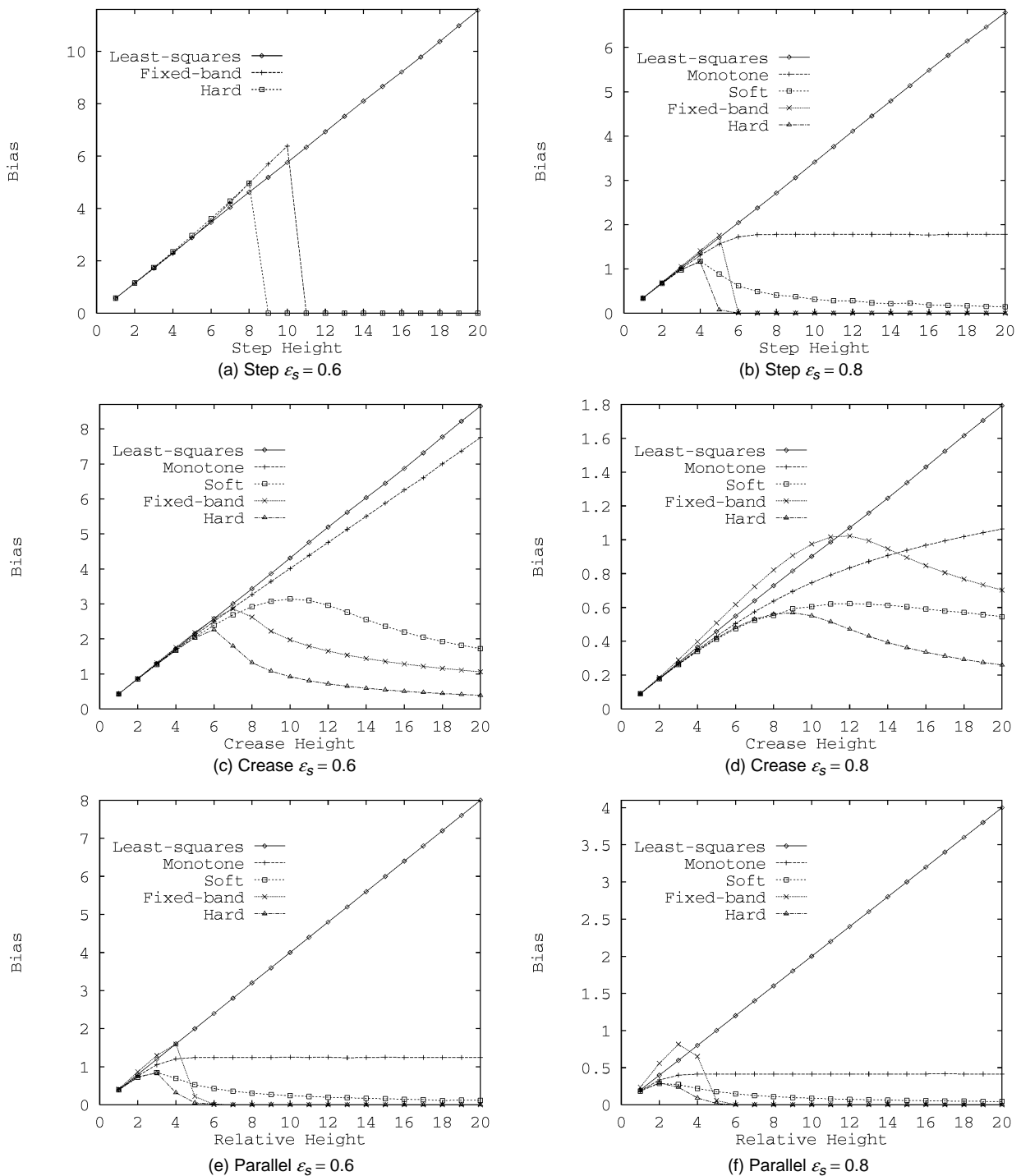


Fig. 7. Bias of fixed-band techniques, fixed-scale M-estimators and least-squares on step edges, (a) and (b), crease edges, (c) and (d), and parallel lines, (e) and (f), as a function of height when  $\varepsilon_s = 0.6$  and  $\varepsilon_s = 0.8$ . The horizontal axis is the relative discontinuity magnitude (height),  $\Delta z/\sigma$ , and the vertical axis is the bias (see (35)). Plots not shown in (a) are essentially equivalent to the least-squares plots.

minimizer of the objective function. Therefore, to avoid local minima, fixed-scale M-estimators should use either a random sampling technique or a Hough transform.

### 6.3 M-Estimators

Next, consider standard M-estimators, which estimate  $\hat{\sigma}$  from the data. To calculate  $T(H)$  for the monotone and soft redescending M-estimators, simply calculate  $\hat{\theta} = T_{p,s}(H)$

for any mixture distribution using (7) or (8) as the objective functional. For the hard redescending M-estimator, which estimates  $\hat{\sigma}$  from an initial fit, the optimum fit to the mixture distribution is found in three stages: First, find the optimum LMS fit, then calculate the median absolute deviation (MAD) [10, p. 107] to this fit, scaling it to estimate  $\hat{\sigma}$ , and, finally, calculate  $\hat{\theta} = T_{p_h}(H)$  with  $\hat{\sigma}$  fixed. Two different scale factors for estimating  $\hat{\sigma}$  are considered: The first, 1.4826,

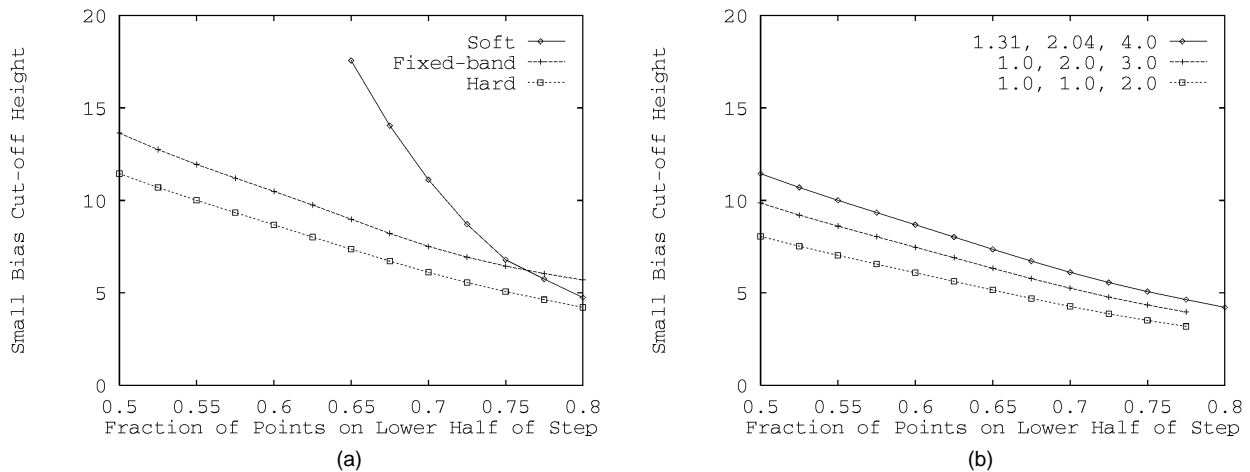


Fig. 8. Small bias cut-off heights as a function of  $\varepsilon_s$ , the relative fraction of points on the lower half of the step. Plots in (a) show the heights for fixed-band techniques and two fixed-scale M-estimators. Plots in (b) show the heights for different tuning parameters of the hard redescending fixed-scale M-estimator. Heights not plotted for small  $\varepsilon_s$  are above  $\Delta z/\sigma = 20$ . When height is not plotted for large  $\varepsilon_s$ , bias is never greater than 1.0.

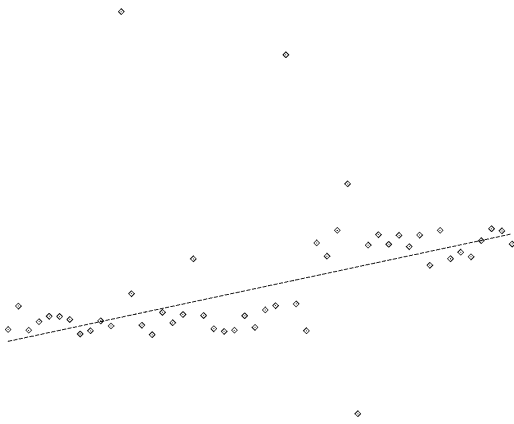


Fig. 9. Example step edge data generated when  $\varepsilon_s = 0.6$  and  $\Delta z/\sigma = 7.5$ , a discontinuity where each of the objective function of each robust estimator (except LTS) is minimized by a biased fit. The example fit shown is  $\hat{\theta}(x)$  for the hard redescending, fixed-scale M-estimator.

ensures consistency at the normal distribution; the second, 1.14601, ensures consistency at Student's  $t$ -distribution (with  $f = 1.5$ ). Using the second allows accurate comparison between the hard redescending M-estimator and the soft redescending M-estimator which is the maximum likelihood estimate for Student's  $t$  distribution [5].

Fig. 10 shows bias plots for the soft redescending M-estimator and for the hard redescending M-estimator using the two different scale factors (plot "Hard-N" for the normal distribution and plot "Hard-t" for the  $t$ -distribution). Results for the monotone M-estimator are not shown since its bias matches that of least-squares almost exactly. Overall, the results are substantially worse than for fixed-scale M-estimators, especially for  $\varepsilon_s = 0.6$ . This is a direct result of  $\hat{\sigma}$  being a substantial over-estimate of  $\sigma$ : for example, when  $\varepsilon_s = 0.6$  and  $\Delta z/\sigma = 10$ ,  $\hat{\sigma}/\sigma \geq 2.4$  for all estimates. (See [22] for analysis of bias in estimating  $\hat{\sigma}$ .) These over-estimates allow a large portion of the residual distribution to fall in the region where  $\rho$  is quadratic, causing the estimator to act more like least-squares. Because of this, M-estimators are heavily biased by discontinuities when they must estimate  $\hat{\sigma}$  from the data.

#### 6.4 LMS, LTS, and MINPRAN

The last estimators examined are LMS, LTS, and MINPRAN, methods which neither require  $\hat{\sigma}$  a priori nor need to estimate it while finding  $\hat{\theta}(x)$ . Fig. 11 shows bias plots for these estimators on step edges, crease edges and parallel lines, using  $\varepsilon_0 = 0.1$  and  $z_0 = 100$ . Fig. 12 shows small bias cut-off heights on step edges for LMS, LTS, and MINPRAN, and it demonstrates the effects of changes in the mixture proportions on LMS and LTS.

LMS and LTS work as well as any technique studied as long as the actual fraction of inliers—data from  $\beta_1(x)$ —is above 0.5. Since this fraction is  $(1 - \varepsilon_0)\varepsilon_s$ , the bias of LMS and LTS, unlike that of M-estimators, depends heavily on both  $\varepsilon_0$  and  $\varepsilon_s$ . (For random sampling implementations of LMS and LTS, where  $p$  points instantiate a hypothesized fit and the objective function is evaluated on the remaining  $n - p$  points, the bias curves in Fig. 11 and the steep drop in cut-off heights in Fig. 12 will shift to the right, but only marginally, since usually  $n \gg p$ .) Figs. 12b and 12c demonstrate this dependence in two ways for LTS. Fig. 12b shows small bias cutoffs as a function of  $\varepsilon_s$ , the relative fraction of inliers points on the lower half of the step. The bias cutoffs are lower for lower  $\varepsilon_0$ , simply because fewer gross outliers imply more actual inliers when  $\varepsilon_s$  remains fixed. Fig. 12c shows small bias cutoffs as a function of the actual fraction of inliers,  $(1 - \varepsilon_0)\varepsilon_s$ . For a fixed fraction of actual inliers, increasing or decreasing  $\varepsilon_0$  decreases or increases the fraction of pseudo outliers the corresponding amount. Thus, comparing the three curves in the plot shows that the coherent structure of the pseudo outliers causes more bias than the random structure of gross outliers. This same effect is shown for LMS in Fig. 12d. Finally, the magnitude of  $z_0$ , which controls the gross outlier distribution, has little effect on the bias results, except in the unrealistic case where it approaches the discontinuity magnitude.

LTS is less biased than LMS, especially when the actual fraction of inliers is only slightly above 0.5. This can be seen most easily by comparing the low bias cutoff plots in Figs. 12c and 12d. Like the advantage of hard redescending M-estimators over fixed-band techniques (Section 6.2), this occurs

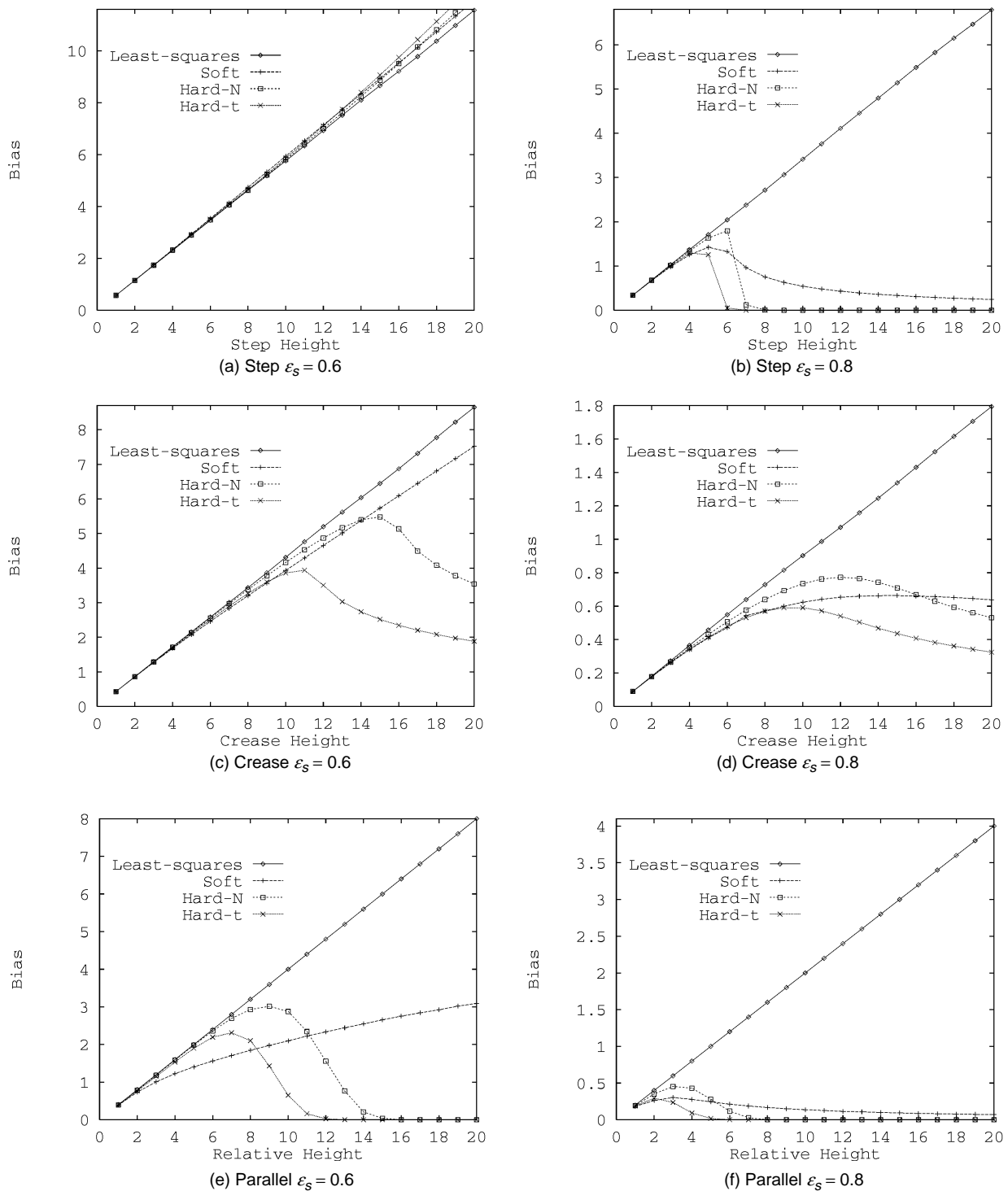


Fig. 10. Bias of M-estimators and least-squares on step edges, (a) and (b), crease edges, (c) and (d), and parallel lines, (e) and (f), when  $\varepsilon_S = 0.6$  and  $\varepsilon_S = 0.8$ . The horizontal axis is the relative discontinuity magnitude (height),  $\Delta z/\sigma$ , and the vertical axis is the bias (see (35)).

because the LTS objective function depends on the smallest 50 percent of the residuals rather than just on the median residual. It is important to note that although the efficiency of LMS can be improved by application of a one-step M-estimator starting from the LMS estimate, this will not substantially improve a heavily biased fit, since a local minimum of the M-estimator objective function will be near this fit.

With a minor modification to its optimization criteria, MINPRAN can be made much less sensitive to pseudo

outliers, improving dramatically on the poor performance shown in Figs. 11 and 12. The idea is to find two disjoint fits (having no shared inliers),  $\hat{\theta}_a$  and  $\hat{\theta}_b$ , with inlier bounds  $\hat{r}_a$  and  $\hat{r}_b$  and inlier counts  $k_{\hat{\theta}_a, \hat{r}_a}$  and  $k_{\hat{\theta}_b, \hat{r}_b}$ , minimizing  $\mathcal{F}(\hat{r}_a + \hat{r}_b, k_{\hat{\theta}_a, \hat{r}_a} + k_{\hat{\theta}_b, \hat{r}_b}, n)$  [23], [26]. If  $\hat{\theta}$  is the single fit minimizing the criterion function, with inlier

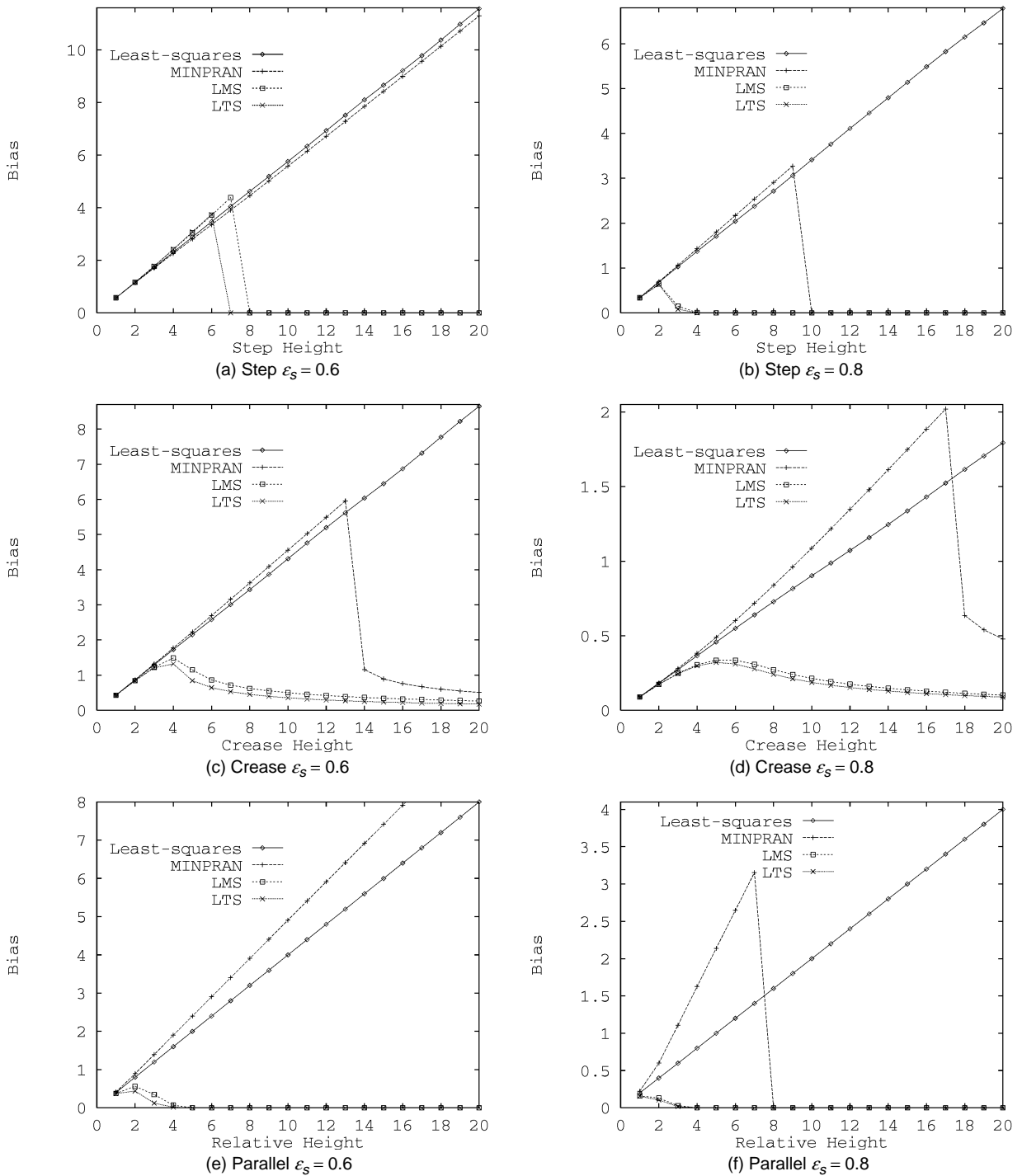


Fig. 11. Bias of MINPRAN, LMS, LTS, and least-squares on step edges, (a) and (b), crease edges, (c) and (d), and parallel lines, (e) and (f), when  $\epsilon_s = 0.6$  and  $\epsilon_s = 0.8$ . The horizontal axis is the relative discontinuity magnitude (height),  $\Delta z/\sigma$ , and the vertical axis is the bias (see (35)).

bound  $\hat{r}$  and inlier count  $k_{\hat{\theta}, \hat{r}}$ , then the two fits  $\hat{\theta}_a$  and  $\hat{\theta}_b$  are chosen instead of the single fit  $\hat{\theta}$  if

$$\mathcal{F}(\hat{r}_a + \hat{r}_b, k_{\hat{\theta}_a, \hat{r}_a} + k_{\hat{\theta}_b, \hat{r}_b}, n) < \mathcal{F}(\hat{r}, k_{\hat{\theta}}, n). \quad (36)$$

Thus, the modified optimization criteria tests whether one or two inlier distributions are more likely in the data [28]. Fig. 12 shows the step edge small bias cut-off heights for this new objective function, denoted by MINPRAN2. These

are substantially lower than those of the other techniques, including LTS. Further, these results, unlike those of MINPRAN, are only marginally affected by the parameters  $\epsilon_o$  and  $z_0$ . Unfortunately, the search for  $\hat{\theta}_a$  and  $\hat{\theta}_b$  is computationally expensive, and so the present implementation of MINPRAN2 uses a simple search heuristic [23], [26] that yields more biased results than the optimum shown here. It is, however, as effective as the fixed-scale, hard re-descending M-estimator and, unlike LMS and LTS, it does not fail dramatically when there are too few inliers.

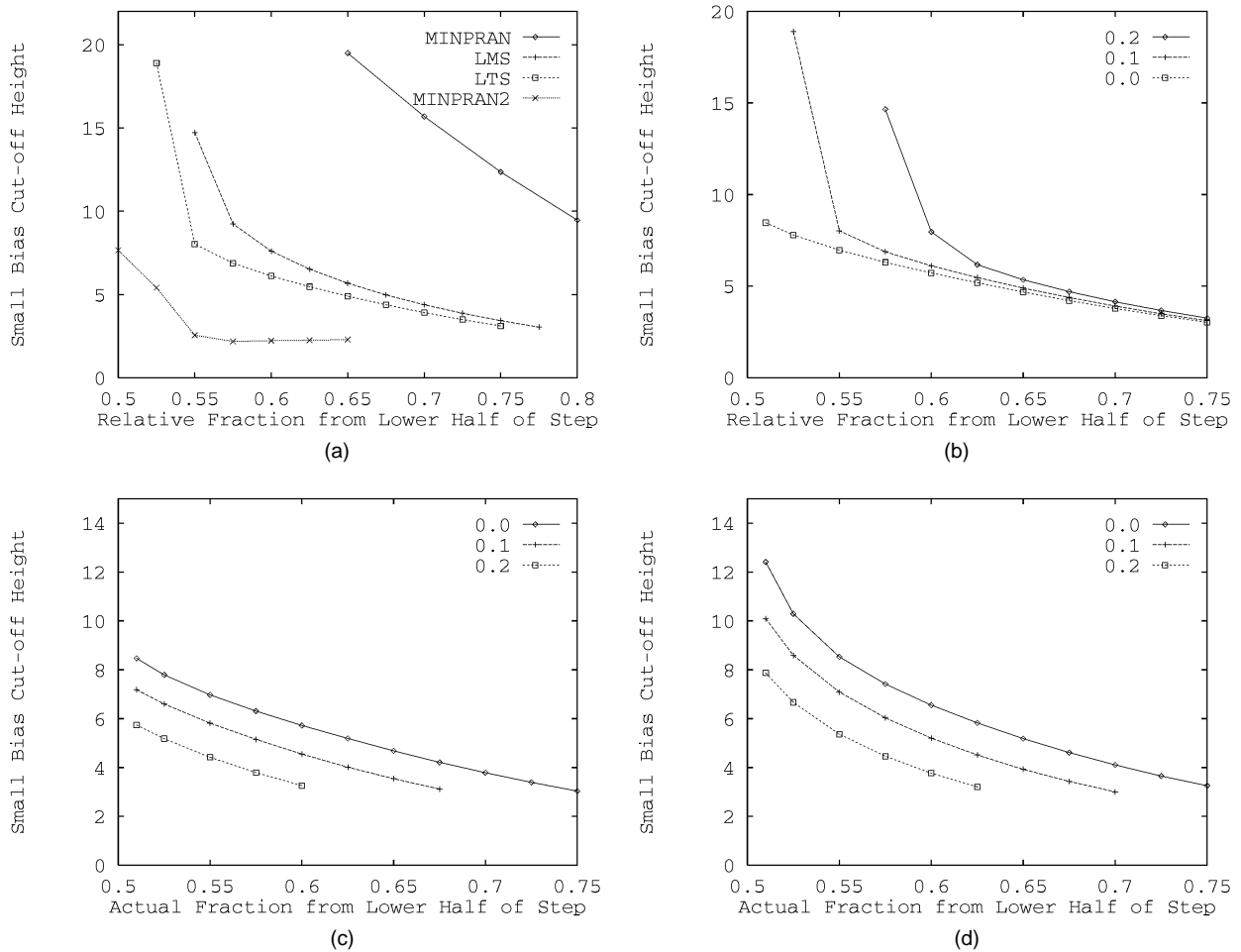


Fig. 12. Small bias cut-off heights. Plot (a) shows these for LMS, LTS, MINPRAN, and the modified MINPRAN optimization criteria (MINPRAN2) as a function of  $\epsilon_s$ , the relative fraction of inliers. Plot (b) shows these for LTS as a function of  $\epsilon_s$  for three different gross outlier percentages  $\epsilon_o$ . Plots (c) and (d) show these for LTS and LMS, respectively, as a function of  $(1 - \epsilon_o)\epsilon_s$ , the actual fraction of inliers for three different gross outlier percentages  $\epsilon_o$ . Heights not plotted for small  $\epsilon_s$  or  $(1 - \epsilon_o)\epsilon_s$  are above  $H/\sigma = 20$ . When height is not plotted for large  $\epsilon_s$  or  $(1 - \epsilon_o)\epsilon_s$ , bias is never greater than  $\sigma$ .

### 6.5 Discussion and Recommendations

Overall, the results show that all the robust estimators studied estimate biased fits at small but substantial discontinuity magnitudes. This bias, which, relative to the bias of least-squares, is greater for crease and step edges and less for parallel lines, occurs even if  $\hat{\sigma}$  or the distribution of gross outliers or both are known a priori. Further, it must be emphasized that *this bias is not an artifact of the search process*: The functional form of each estimator returns the fit corresponding to the global minimum of the estimator's objective function.

The reason for the bias can be seen by examining the cumulative distribution functions (cdfs) of absolute residuals. Fig. 13 plots this cdf,  $F^a(r|\theta, H)$ , when  $\theta$  is the target fit ( $\theta = \beta_j$ ) and, when  $\theta$  is the least-squares fit to  $H$ , for  $H$  modeling crease and step discontinuities. For  $\Delta z/\sigma = 6.0$ , the cdf of the biased fit is almost always greater than that of the target fit, meaning that in a discrete set of samples the biased fit, which crosses through both point sets, will on average yield smaller magnitude residuals than the target fit, which is close to only the target point set. (The situation is somewhat better when  $\Delta z/\sigma = 9.0$ .) Therefore, robust estimators, such as the ones studied, whose objective functions are based solely on residuals, are unlikely to estimate unbiased fits at small magnitude discontinuities.

While none of the estimators works as well as desired, the following recommendations for choosing among them are based on the results presented above:

- When  $\hat{\sigma}$  is known a priori, one should use a hard re-descending M-estimator objective function, such as Hampel's, with reduced tuning parameter values and either a random-sampling search technique or a weighted Hough transform. To ensure all inliers are found and to obtain greater statistical efficiency, a one-step M-estimator with larger tuning parameters should be run from the initial optimum fit. This technique is preferable to LTS and LMS because it is less sensitive to the number of gross outliers.
- When  $\hat{\sigma}$  is not known a priori, but the distribution of gross outliers is known, one should use the modified MINPRAN algorithm, MINPRAN2 [23], [26].
- When neither  $\hat{\sigma}$  nor the distribution of gross outliers is known, LTS should be used, although its performance degrades quickly when there are too few inliers. LTS is preferable to LMS because of its statistical efficiency.

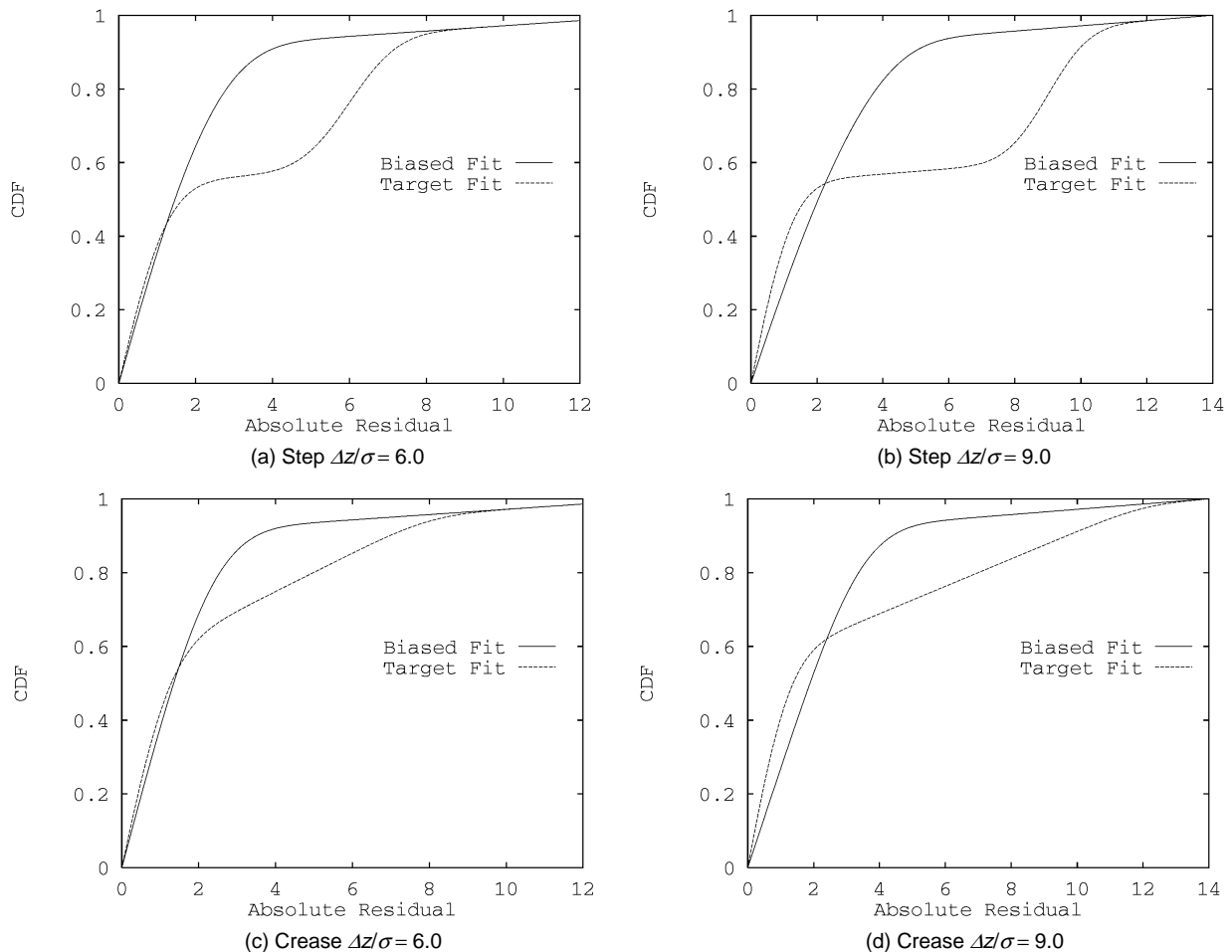


Fig. 13. Each figure plots the cumulative distribution functions (cdf) of absolute residuals for the target fit and for a biased (least-squares) fit: (a) and (b) are relative to a step discontinuity, and (c) and (d) are relative to a crease discontinuity. For all plots, the mixture fractions are fixed at  $\epsilon_o = 0.1$  and  $\epsilon_s = 0.6$ . All robust estimators are substantially biased at  $\Delta z/\sigma = 6.0$  for both step and crease discontinuities.

## 7 SUMMARY AND CONCLUSIONS

This paper has developed the pseudo outlier bias metric using techniques from mathematical statistics to study the fitting accuracy of robust estimators on data taken from multiple structures—surface discontinuities, in particular. Pseudo outlier bias measures the distance between a robust estimator's optimum fit to a target distribution and its optimum fit to an outlier corrupted mixture distribution. Here, the target distribution models the points from a single surface and the mixture distribution models points from multiple surfaces plus gross outliers. The optimum fit for each estimator is found by applying its functional form to one of these model distributions. Thus, like other analysis tools from the robust statistics literature, pseudo outlier bias depends on point distributions rather than on particular point sets drawn from these distributions. While this has some limitations—the actual fitting error for particular point sets may be more or less than the pseudo outlier bias and it ignores problems that may arise from multiple local minima in an objective function—it represents a simple, efficient, and elegant method of analyzing robust estimators.

Pseudo outlier bias was used to analyze the performance of M-estimators, fixed-band techniques (Hough transforms and RANSAC), least median of squares (LMS), least

trimmed squares (LTS), and MINPRAN in fitting surfaces to three different discontinuity models: step edges, crease edges, and parallel lines. For each of these discontinuities, two surfaces generate data, with the larger set of surface data forming the inliers and the smaller set forming the pseudo outliers. By characterizing these discontinuity models using a small number of parameters, formulating the models as mixture distributions, and studying the bias of the robust estimators as the parameters varied, it was shown that each robust estimator is biased for substantial discontinuity magnitudes. This effect, which relative to that of least-squares, is strongest for step edges and crease edges, persists even when the noise in the data or the gross outlier distribution or both are known in advance. It is disappointing because in vision data—not just in range data—multiple structures (pseudo outliers) are more prevalent than gross outliers. In spite of the disappointment, however, specific recommendations, which depend on what is known about the data, were made for choosing between current techniques.<sup>4</sup>

These negative results indicate that care should be taken when using robust techniques to estimate surface parameters from range data—either to obtain local low-order sur-

4. See [14], [17] for new, related techniques.

face approximations or to initialize fits for surface growing algorithms [3], [5], [6], [15]. Similar difficulties may occur for the "layers" techniques that have been applied to motion analysis [1], [6], [29] and for other estimation problems where multiple structures may be "near" each other in the data. In range data applications, robust estimates will be accurate for large scale depth discontinuities and sharp corners, but will be skewed at small magnitude discontinuities, such as near the boundary of a slightly raised or depressed area of a surface or near a moderate change in surface orientation. Obtaining accurate estimates near these discontinuities will require new and perhaps more sophisticated robust estimators.

## ACKNOWLEDGMENTS

The author would like to acknowledge the financial support of the U.S. National Science Foundation under grants IRI-9217195 and IRI-9408700, the assistance of James Miller in various aspects of this work, and the insight offered by the anonymous reviewers which led to substantial improvements in the presentation. This paper presents a substantial reformulation and improvement of an earlier version of this work, which was described in [25].

## REFERENCES

- [1] S. Ayer and H. Sawhney, "Layered Representation of Motion Video Using Robust Maximum Likelihood Estimation of Mixture Models and MDL Encoding," *Proc. IEEE Int'l Conf. Computer Vision*, pp. 777-784, 1995.
- [2] P.J. Besl, J.B. Birch, and L.T. Watson, "Robust Window Operators," *Proc. IEEE Int'l Conf. Computer Vision*, pp. 591-600, 1988.
- [3] P.J. Besl and R.C. Jain, "Segmentation Through Variable-Order Surface Fitting," *IEEE Trans. Pattern Analysis and Machine Intelligence*, vol. 10, pp. 167-192, 1988.
- [4] R.C. Bolles and M.A. Fischler, "A Ransac-Based Approach to Model Fitting and Its Application to Finding Cylinders in Range Data," *Proc. Seventh Int'l Joint Conf. Artificial Intelligence*, pp. 637-643, 1981.
- [5] K.L. Boyer, M.J. Mirza, G. Ganguly, "The Robust Sequential Estimator: A General Approach and Its Application to Surface Organization in Range Data," *IEEE Trans. Pattern Analysis and Machine Intelligence*, vol. 16, pp. 987-1001, 1994.
- [6] T. Darrell and A. Pentland, "Cooperative Robust Estimation Using Layers of Support," *IEEE Trans. Pattern Analysis and Machine Intelligence*, vol. 17, pp. 474-487, 1995.
- [7] M.A. Fischler and R.C. Bolles, "Random Sample Consensus: A Paradigm for Model Fitting with Applications to Image Analysis and Automated Cartography," *Comm. ACM*, vol. 24, pp. 381-395, 1981.
- [8] J.D. Gaskill, *Linear Systems, Fourier Transforms, and Optics*. New York: John Wiley and Sons, 1978.
- [9] F.R. Hampel, P.J. Rousseeuw, and E. Ronchetti, "The Change-of-Variance Curve and Optimal Redescending M-Estimators," *J. Am. Statistical Assoc.*, vol. 76, pp. 643-648, 1981.
- [10] F.R. Hampel, P.J. Rousseeuw, E. Ronchetti, and W.A. Stahel, *Robust Statistics: The Approach Based on Influence Functions*. New York: John Wiley & Sons, 1986.
- [11] P.W. Holland and R.E. Welsch, "Robust Regression Using Iteratively Reweighted Least-Squares," *Communications of Statistics-Theoretical Methods*, vol. A6, pp. 813-827, 1977.
- [12] P.J. Huber, *Robust Statistics*. New York: John Wiley & Sons, 1981.
- [13] J. Illingworth and J. Kittler, "A Survey of the Hough Transform," *Computer Vision, Graphics, and Image Processing*, vol. 44, pp. 87-116, 1988.
- [14] K.-M. Lee, P. Meer, and R.-H. Park, "Robust Adaptive Segmentation of Range Images," *IEEE Trans. Pattern Analysis and Machine Intelligence*, to appear.
- [15] A. Leonardis, A. Gupta, and R. Bajcsy, "Segmentation of Range Images as the Search for Geometric Parametric Models," *Int'l J. Computer Vision*, vol. 14, pp. 253-277, 1995.
- [16] P. Meer, D. Mintz, A. Rosenfeld, and D.Y. Kim, "Robust Regression Methods for Computer Vision: A Review," *Int'l J. Computer Vision*, vol. 6, pp. 59-70, 1991.
- [17] J.V. Miller and C.V. Stewart, "MUSE: Robust Surface Fitting Using Unbiased Scale Estimates," *Proc. IEEE Conf. Computer Vision and Pattern Recognition*, pp. 300-306, 1996.
- [18] M.J. Mirza and K.L. Boyer, "Performance Evaluation of a Class of M-Estimators for Surface Parameter Estimation in Noisy Range Data," *IEEE Trans. Robotics and Automation*, vol. 9, pp. 75-85, 1993.
- [19] W.H. Press, S.A. Teukolsky, W.T. Vetterling, and B.P. Flannery, *Numerical Recipes in C: The Art of Scientific Computing*. Cambridge Univ. Press, 1992.
- [20] G. Roth and M.D. Levine, "Extracting Geometric Primitives," *Computer Vision, Graphics, and Image Processing: Image Understanding*, vol. 58, pp. 1-22, 1993.
- [21] P.J. Rousseeuw, "Least Median of Squares Regression," *J. Am. Statistical Assoc.*, vol. 79, pp. 871-880, 1984.
- [22] P.J. Rousseeuw and C. Croux, "Alternatives to the Median Absolute Deviation," *J. Am. Statistical Assoc.* vol. 88, pp. 1,273-1,283, 1993.
- [23] C.V. Stewart, "A New Robust Operator for Computer Vision: Application to Range Images," *Proc. IEEE Conf. Computer Vision and Pattern Recognition*, pp. 167-173, 1994.
- [24] C.V. Stewart, "A New Robust Operator for Computer Vision: Theoretical Analysis," *Proc. IEEE Conf. Computer Vision and Pattern Recognition*, pp. 1-8, 1994.
- [25] C.V. Stewart, "Expected Performance of Robust Estimators Near Discontinuities," *Proc. IEEE Int'l Conf. Computer Vision*, pp. 969-974, 1995.
- [26] C.V. Stewart, "MINPRAN: A New Robust Estimator for Computer Vision," *IEEE Trans. Pattern Analysis and Machine Intelligence*, vol. 17, pp. 925-938, 1995.
- [27] C.V. Stewart, "Bias in Robust Estimation Caused by Discontinuities and Multiple Structures," Technical Report 96-4, Dept. of Computer Science, Rensselaer Polytechnic Inst. (see also <http://www.cs.rpi.edu/~stewart>), 1996.
- [28] D.M. Titterton, A.F.M. Smith, and U.E. Makov, *Statistical Analysis of Finite Mixture Distributions*. New York: John Wiley and Sons, 1985.
- [29] J.Y.A. Wang and E.H. Adelson, "Layered Representation for Motion Analysis," *Proc. IEEE Conf. Computer Vision and Pattern Recognition*, pp. 361-366, 1993.



**Charles V. Stewart** (M '88) received the BA degree in mathematical sciences from Williams College in 1982, and the MS and PhD degrees in computer science from the University of Wisconsin in 1985 and 1988, respectively. Currently, he is an associate professor in the Department of Computer Science, Rensselaer Polytechnic Institute, Troy, New York. During the 1996-97 academic year, he spent a sabbatical at the GE Center for Research and Development in Niskayuna, New York. He is a member of the ACM and the IEEE. His research interests include computer vision, robust statistics, and computational geometry.